

## Alignment of the HTLV-I Rex Peptide Bound to Its Target RNA Aptamer from Magnetic Field-Induced Residual Dipolar Couplings and Intermolecular Hydrogen Bonds

Hashim M. Al-Hashimi,\* Andrey Gorin,  
Ananya Majumdar, and Dinshaw J. Patel

Cellular Biochemistry and Biophysics Program  
Memorial Sloan-Kettering Cancer Center  
New York, New York 10021

Received December 1, 2000

Revised Manuscript Received January 17, 2001

Structure determination of molecular complexes by NMR has traditionally relied on distance constraints derived from the measurement of the intermolecular nuclear Overhauser effects (NOEs).<sup>1</sup> The success of this approach, however, relies on having a large number of observable, assignable, and proximal (<6 Å) proton resonances at the binding interface. Even under conditions where the above requirements are well met, assignment of intermolecular NOEs is a time-consuming process,<sup>2</sup> which has important implications for the scope of NMR in rational drug design efforts.<sup>3</sup> This communication is concerned with an alternative NMR approach for structure determination of nucleic acid complexes,<sup>4,5</sup> which relies on a combination of magnetic field-induced residual dipolar couplings ( $D$ ) for long-range orientational constraints,<sup>6–9</sup> and  $^2\text{h}J_{\text{NN}}$  correlated spectroscopy for intermolecular hydrogen-bonding constraints.<sup>10,11</sup> We demonstrate that the alignment of a 16-mer HTLV-1 Rex peptide bound to a 33-mer RNA aptamer, for which a high-resolution NOE-based structure has previously been reported,<sup>12</sup> can be determined using only these intermolecular constraints.

Our approach shares similarities with previous studies by Prestegard and co-workers on the protein-bound geometry of a carbohydrate molecule,<sup>13</sup> and with one of the original dipolar couplings studies by Tjandra et. al. on the field-aligned GATA-1–DNA complex.<sup>7</sup> Given five or more independent residual dipolar couplings measured between nuclei within the peptide and RNA, and knowledge of their individual molecular structures, relative molecular orientation can be established by determining and superimposing molecule-centered order tensor frames.<sup>14,15</sup> For magnetic field alignment of nucleic acids, the

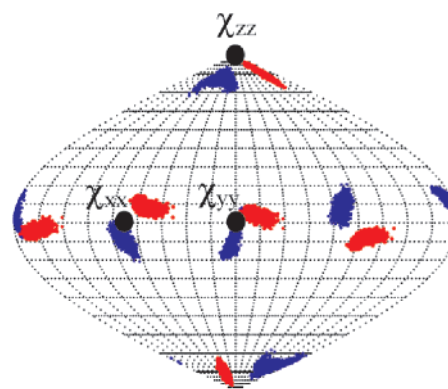


**Figure 1.** Sauson–Flaumsted projection map<sup>20</sup> depicting principal diamagnetic susceptibility orientational solutions for the RNA/peptide complex. In black filled circles, calculated orientational solutions ( $\chi^{\text{calc}}$ ) using a tensor summation of individual base group anisotropies<sup>18</sup> and their relative geometry from the high-resolution NMR structure (PDB 1c4j), as previously described.<sup>6,7</sup> In blue, orientational solutions for the RNA ( $\chi^{\text{RNA}}$ ) determined using seven residual dipolar couplings between directly bonded H1–N1 in guanine and H3–N3 in uracil (residues G8, G9, U10, G13, U18, G24, G29; Table S1), coordinates for the RNA from the NMR structure (PDB 1c4j) rotated into the calculated  $\chi^{\text{calc}}$ -tensor frame, and using the program ODERTEN\_SVD.<sup>15</sup> In red, orientational solutions for the bound peptide determined using six  $^1D_{\text{NH}}$  (residues R5, R7, R9, R10, S11, and R13) and three  $^1D_{\text{C}\alpha\text{H}\alpha}$  (residues R5, Q12, and R13) residual dipolar couplings measured in the core of the peptide (residues 5–13 inclusive; Table S1), coordinates for the peptide determined in the absence of intermolecular NOEs (see main text), and the program ORDERTEN\_SVD.<sup>15</sup> Values for magnetic susceptibility anisotropy ( $\Delta\chi$  in  $\text{m}^3/\text{molecule} \times 10^{-34}$ ) and asymmetry ( $\eta = |(\chi_{yy} - \chi_{xx})/\chi_{zz}|$ ) were  $\Delta\chi^{\text{calc}} = -292/-371$  and  $\eta^{\text{calc}} = 0.12/0.44$  (for a family of 12 RNA structures previously determined by NMR);  $\Delta\chi^{\text{RNA}} = -371/-475$  and  $\eta^{\text{RNA}} = 0.53 \leftrightarrow 0.95$ ;  $\Delta\chi^{\text{pep}} = -368/-490$ ,  $\eta^{\text{pep}} = 0.36/0.59$ . The departure from axial symmetry ( $\eta \neq 0$ ) is attributed to the L-shaped conformation of the RNA aptamer (see Figure 2). NMR experiments on the RNA and peptide were acquired on uniformly [ $^{15}\text{N}/^{13}\text{C}$ RNA/ $^{15}\text{N}/^{13}\text{C}$ -peptide] and [unlabeledRNA/ $^{15}\text{N}/^{13}\text{C}$ -peptide]-labeled samples, respectively. One bond  $^1\text{H}$ – $^{15}\text{N}$  splittings were measured using the SCE-HSQC experiment,<sup>21</sup> and splittings were extracted using a Bayesian time-domain NMR parameter estimation program Xrambo<sup>22</sup> as previously described.<sup>13</sup> One bond  $^1\text{H}\alpha$ – $^{13}\text{C}\alpha$  splittings in the peptide were measured using the intensity-based  $^1J_{\text{CH}}$ -modulated CT-HSQC experiment.<sup>23</sup> In all cases, field-induced residual dipolar couplings at 800 MHz were computed using splittings measured at 500 and 800 MHz, and using the quadratic field dependence ( $B^2$ ) of dipolar couplings as previously described.<sup>6</sup>

diamagnetic susceptibility tensor ( $\chi$ ) frame can be directly computed, provided there is knowledge of the molecular structure.<sup>7,16–18</sup>

In Figure 1, we compare principal orientational solutions for the RNA  $\chi$ -tensor (black filled circles) calculated on the basis of individual values of base group magnetic susceptibility anisotropies ( $\chi^{\text{calc}}$ ),<sup>18</sup> with orientational solutions (in blue) determined using seven  $^1D_{\text{NH}}$  residual dipolar couplings (Table S1) measured between nuclei in the bases of the RNA,<sup>15</sup> partially aligned under the influence of 18.7 T magnetic field ( $\chi^{\text{RNA}}$ ).<sup>18</sup> Orientational solutions are depicted relative to the same molecular frame, and

\* Author for correspondence. Telephone (212)-639-7225. Fax: (212) 717-3453. E-mail: hashimi@sbnmr1.mskcc.org.

(1) Wüthrich, K. *NMR of Proteins and Nucleic Acids*; Wiley: New York, 1986.

(2) Clore, G. M. *Proc. Natl. Acad. Sci. U.S.A.* **2000**, *97*, 9021–9025.

(3) Huang, X. M.; Moy, F.; Powers, R. *Biochemistry* **2000**, *39*, 13365–13375.

(4) Lynch, S. R.; Puglisi, J. D. *J. Am. Chem. Soc.* **2000**, *122*, 7853–7854.

(5) Mollova, E. T.; Hansen, M. R.; Pardi, A. *J. Am. Chem. Soc.* **2000**, *122*, 11561–11562.

(6) Tolman, J. R.; Flanagan, J. M.; Kennedy, M. A.; Prestegard, J. H. *Proc. Natl. Acad. Sci. U.S.A.* **1995**, *92*, 9279–9283.

(7) Tjandra, N.; Omichinski, J. G.; Gronenborn, A. M.; Clore, G. M.; Bax, A. *Nat. Struct. Biol.* **1997**, *4*, 732–738.

(8) Prestegard, J. H.; Tolman, J. R.; Al-Hashimi, H. M.; Andrec, M. In *Biological Magnetic Resonance*; Krishna, N. R., Berliner, L. J., Eds.; Plenum: New York, 1999; Vol. 17, pp 311–355.

(9) Bayer, P.; Varani, L.; Varani, G. *J. Biomol. NMR* **1999**, *14*, 149–155.

(10) (a) Dingley, A. J.; Grzesiek, S. *J. Am. Chem. Soc.* **1998**, *120*, 8293–8297. (b) Pervushin, K.; Fernandez, C.; Szyperski, T.; Kainosho, M.; Wüthrich, K. *Proc. Natl. Acad. Sci. U.S.A.* **1998**, *95*, 14147–14151.

(11) Liu, A.; Majumdar, A.; Jiang, F.; Chernichenko, N.; Skripkin, E.; Patel, D. J. *J. Am. Chem. Soc.* **2000**, *122*, 11226–11227.

(12) Jiang, F.; Gorin, A.; Hu, W.; Majumdar, A.; Baskerville, S.; Xu, W.; Ellington, A.; Patel, D. J. *Struct. Folding Des.* **1999**, *7*, 1461–1472.

(13) (a) Bolon, P. J.; Al-Hashimi, H. M.; Prestegard, J. H. *J. Mol. Biol.* **1999**, *293*, 107–115. (b) Al-Hashimi, H. M.; Bolon, P. J.; Prestegard, J. H. *J. Magn. Reson.* **2000**, *142*, 153–158.

(14) Saupe, A. Z. *Naturforsch.* **1964**, *19a*, 161.

(15) Losonczi, J. A.; Andrec, M.; Fischer, M. W. F.; Prestegard, J. H. *J. Magn. Reson.* **1999**, *138*, 334–342.

(16) Tolman, J. R.; Flanagan, J. M.; Kennedy, M. A.; Prestegard, J. H. *Nat. Struct. Biol.* **1997**, *4*, 292–297.

(17) Al-Hashimi, H. M.; Majumdar, A.; Gorin, A.; Kettani, A.; Skripkin, E.; Patel, D. J. *J. Am. Chem. Soc.* **2001**, *123*, 633–640.

(18) (a) Bastiaan, E. W.; MacLean, C. *NMR* **1990**, *25*, 17–43. (b) Bothner-By, A. A. In *Encyclopedia of Nuclear Magnetic Resonance*; Grant, D. M., Harris, R. K., Eds.; Wiley: Chichester, 1995; pp 2932–2938.

using coordinates for the RNA aptamer from the previous NMR structure (PDB 1c4j). As shown in Figure 1, all three experimentally determined orientational solutions are in very good agreement with calculated values<sup>1</sup>, with a minimum deviation of  $\sim 7^\circ$ .

To determine the RNA/peptide alignment, the  $\chi$ -tensor frame needs to be determined from the point of view of the bound peptide ( $\chi^{(\text{pep})}$ ). However, this determination requires knowledge of the peptide bound geometry, which can be more critically dependent on the availability of distance constraints from intermolecular NOE contacts. The peptide structure was therefore re-determined using only 11 dihedral and 276 *intra* peptide-NOE restraints. A family of 12 lowest-energy peptide structures was subsequently tested for consistency with nine backbone residual dipolar couplings (*five*  $^1D_{\text{NH}}$  and *four*  $^1D_{\text{CaHa}}$ , Table S1) measured in the core of the peptide (residues 5–13 inclusively) using an order tensor calculation. The orientational solutions determined using coordinates from the “best fit” peptide geometry (rmsd between calculated and measured couplings  $\sim 0.8$  Hz for  $^1D_{\text{NH}}$  and 1.2 Hz for  $^1D_{\text{CaHa}}$ ) and residual dipolar couplings are shown in Figure 1 in blue ( $\chi^{(\text{pep})}$ ).

In Figure 2, we show the peptide alignment (in gray) relative to the RNA aptamer (in blue) determined by superimposing the centers of the experimentally determined  $\chi$ -tensor frames ( $\chi^{(\text{RNA})}$  and  $\chi^{(\text{pep})}$ ). While this leads to four possible RNA/peptide alignments due to allowed inversion about principal axes ( $\chi_{xx}$ ,  $\chi_{yy}$ ,  $\chi_{zz}$ ),<sup>19</sup> three of these could be discarded by the need to satisfy three intermolecular hydrogen-bonding interactions between arginine side-chain guanidinium groups ( $^{\eta}\text{NH}_2$ ) and N7 nitrogens of guanine bases, for residue pairs R5–G8, R7–G24, and R13–G25, shown in Figure 2 as purple, green, and yellow residues, respectively. These intermolecular hydrogen bonds, which were previously measured directly via  $^2hJ_{\text{NN}}$  couplings,<sup>11</sup> could also be used to guide translation of the determined peptide alignment into the major groove of the RNA aptamer ( $\text{N}_\eta \cdots \text{N7}$  distance  $< 3.0$  Å). As shown in Figure 2, while hydrogen bonds between R7–G24 (in green) and R13–G25 (in yellow) could be satisfied through translation of the determined peptide alignment, deviations in the side chain conformation of residue R5 does not allow for direct hydrogen-bonding interactions with residue G8 in the RNA aptamer. Hydrogen bonding between these residues could, however, be restored by a simple rearrangement of the side-chain conformation of residue R5 (Figure 2). For comparison, the peptide alignment from the NMR structure determined using 189 intermolecular NOE-based distance constraints is also shown in Figure 2 (red peptide). The two peptide alignments are in very good agreement, with deviations in relative peptide/RNA orientations being less than  $15^\circ$ , and with primary deviations being in residues R5 and R6 within the peptide, which displayed high rmsd values in the previous high-resolution NMR structure (1.8 Å and 2.7 Å respectively).<sup>12</sup>

In conclusion, residual dipolar couplings provide decisive orientational constraints on the alignment of two molecules in a complex.<sup>2</sup> In cases where hydrogen-bond mediated scalar couplings are difficult to detect, a small number of intermolecular NOEs can also be used to provide the distance constraints needed

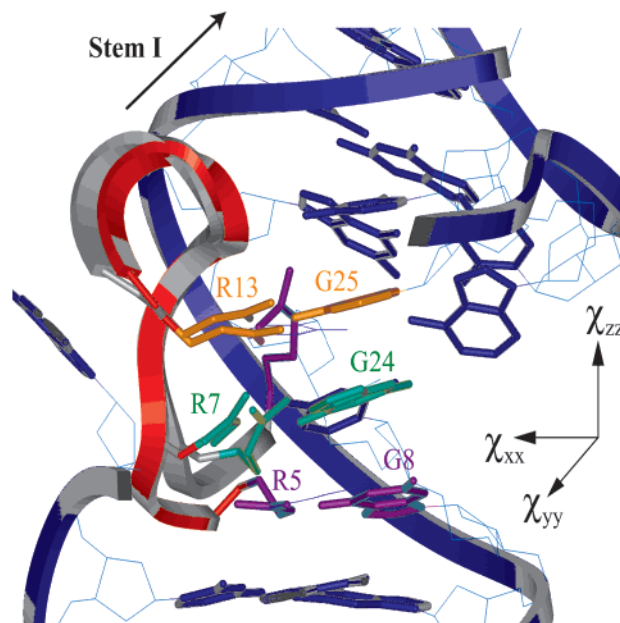


**Figure 2.** RNA/peptide alignment. In gray, the alignment of the core region of the peptide (residues 5–13) relative to the RNA aptamer (in blue) determined by superimposing *experimentally* determined RNA and peptide  $\chi$ -tensor frames, and by translating the peptide orientation to satisfy three intermolecular hydrogen bonding interactions between  $^{\eta}\text{-NH}_2$  protons in the peptide and N7 nitrogens in the RNA. Hydrogen-bonding interactions are readily satisfied for residue pairs R7–G24 and R13–G25 shown in green and yellow respectively, while deviations in the side-chain conformation for residue R5 (shown in purple) does not allow direct hydrogen-bonding interactions with residue G8. This hydrogen-bonding interaction can be restored by a simple rearrangement of the R5 side-chain conformation. For comparison, the peptide alignment from the previous intermolecular NOE-based NMR structure<sup>12</sup> is shown in red. Alignments are depicted relative to the *experimentally* determined RNA  $\chi^{(\text{RNA})}$ -tensor frame. Both the calculated and experimentally determined direction of principal order ( $\chi_{zz} < 0$ ) points along the *effective* long axis of the L-shaped RNA aptamer,<sup>12</sup> and direction of lowest order ( $\chi_{xx} > 0$ ) along the direction defined by the inclination of stem 1.

for docking two molecules in a complex, as recently demonstrated by Clore for a protein–protein complex.<sup>2</sup> Finally, for a target nucleic acid with a known structure,  $\chi$ -tensor frames can reliably be calculated when using magnetic field alignment, obviating the need for dipolar data on the nucleic acid, and application can therefore be extended to larger systems where a favorable increase in alignment can be expected. Hence, field alignment can have distinct advantages, as we showed here in our study of an “S”-shaped peptide bound to an “L”-shaped RNA aptamer.

**Acknowledgment.** We thank Dr. James H. Prestegard (University of Georgia) and Dr. Erick R. P. Zuiderweg (University of Michigan) for 800 MHz time. We thank Dr. Feng Jiang, Dr. Eugene Skripkin, and Ms. Natalya Chernichenko for sample preparation, and Dr. J. Tolman for the  $\chi$ -tensor program. Supported by NIH Grant CA 49982 to D.J.P..

**Supporting Information Available:** Table of measured dipolar couplings (PDF). This material is available free of charge via the Internet at <http://pubs.acs.org>.

(19) Al-Hashimi, H. M.; Valafar, H.; Terrell, M.; Zartler, E. R.; Eidsness, M. K.; Prestegard, J. H. *J. Magn. Reson.* **2000**, *143*, 402–406.

(20) Bugayevskiy, L. M.; Snyder, J. P. *Map Projections: A Reference Manual*; Taylor & Francis: London, 1995.

(21) Tolman, J. R.; Prestegard, J. H. *J. Magn. Reson., Ser. B* **1996**, *112*, 269–274.

(22) Andrec, M.; Prestegard, J. H. *J. Magn. Reson.* **1998**, *130*, 217–232.

(23) Tjandra, N.; Bax, A. *J. Magn. Reson.* **1997**, *124*, 512–515.